Journal of Microbiological Methods 184 (2021) 106201

Contents lists available at ScienceDirect

Journal of Microbiological Methods

journal homepage: www.elsevier.com/locate/jmicmeth

Development and validation of a high-content screening assay for inhibitors of enteropathogenic *E. coli* adhesion

Tuomas Pylkkö, Polina Ilina, Päivi Tammela *

Drug Research Program, Division of Pharmaceutical Biosciences, Faculty of Pharmacy, P.O. Box 56, FI-00014, University of Helsinki, Finland

ARTICLE INFO

Keywords:
Antivirulence drug discovery
Enteropathogenic *E. coli*
Fluorescence microscopy
High-content screening
A/E lesion
T3SS

ABSTRACT

Enteropathogenic *E. coli* (EPEC) causes intestinal infections leading to severe diarrhea. EPEC attaches to the host cell causing lesions to the intestinal epithelium coupled with the effacement of microvilli. In the process, actin accumulates into a pedestal-like structure under bacterial microcolonies. We designed an automated fluorescence microscopy-based screening method for discovering compounds capable of inhibiting EPEC adhesion and virulence using aurodox, a type three secretion system (T3SS) inhibitor, as a positive control. The screening assay employs an EPEC strain (2348/69) expressing a fluorescent protein and actin staining for monitoring the bacteria and their pedestals respectively, analyzing these with a custom image analysis pipeline. The assay allows for the discovery of compounds capable of preventing the formation of pathogenic actin rearrangements. These compounds may be interfering with virulence-related molecular pathways relevant for developing antivirulence leads.

1. Introduction

Gastrointestinal infections and diarrheal diseases are pervasive global health burdens, especially with ever-increasing levels of antimicrobial drug resistance (Fagundes-Neto, 2013). One considerable cause of diarrhea and intestinal infections is enteropathogenic *Escherichia coli* (EPEC), which exhibits resistance to a large range of antibiotics (Rodrigues, 2019; Eltai et al., 2020). Treating resistant gastrointestinal infections with antibiotics is particularly problematic because antibiotics also target protective normal flora, while possibly not eliminating resistant pathogens. As a consequence, an extensive amount of research has been put forward to develop so-called antivirulence drugs, that is, drugs capable of attenuating virulence, without eliminating bacteria (see Dickey et al., 2017 for review). Approved antivirulence drugs to date are compounds attenuating the effects of toxins, but preclinical research has also focused at other possible targets, such as various attachment adhesins and appendices, cell-to-cell communication (quorum sensing), inhibition of specialized bacterial secretory systems, and virulence gene expression (Buroni and Chiarelli, 2020; Theuretzbacher et al., 2020).

The virulence of EPEC, and many other human enteric pathogens is brought about by manipulating pathways of membrane trafficking, cell death/survival and the modulation of the cytoskeleton, ultimately altering the macroscopic properties of the epithelium and provoking gastroenteritis (Mattoo et al., 2007). So-called effector proteins (virulence factors) are used by EPEC and most Gram-negative pathogens to achieve these effects. Effector proteins are injected into the host cell using the type three secretion system (T3SS), a needle-like injection appendage and associated effectors (Gophna et al., 2003). The effectors are typically carried through the needle by chaperones to the cytosol where they play various roles, often aiding the pathogen in invading the host and surviving host defense mechanisms. The size of the ensemble of secreted effectors varies between pathogens, from the four of *Pseudomonas aeruginosa* to several hundred in other pathogens (Lee et al., 2005). Due to the near universality of the T3SS, research has targeted this system in attempts to discover drugs capable of attenuating virulence without antibiotic mechanisms of action (Baron, 2010). The most advanced demonstration of the therapeutic usefulness of T3SS inhibition has been a phase 2 trial of an antibody for *Pseudomonas aeruginosa* infections by KaloBios Pharmaceuticals (Jain et al., 2018).

In typical presentations of EPEC infection, the bacterium adheres to intestinal epithelium, causing the localized effacement of microvilli, the

Abbreviations: A/E, attaching and effacing; EPEC, enteropathogenic *Escherichia coli*; LEE, locus of enterocyte effacement; T3SS, type III secretion system; HTS, high-throughput screening..

* Corresponding author.
E-mail address: paivi.tammela@helsinki.fi (P. Tammela).

https://doi.org/10.1016/j.mimet.2021.106201
Received 5 February 2021; Received in revised form 5 March 2021; Accepted 5 March 2021
Available online 10 March 2021

abnormal polymerization of actin in its vicinity, and increasing the permeability of the epithelium (Moon et al., 1983). Initially EPEC adheres to cells using multiple appendices (e.g. pili) forming localized bacterial aggregates or microcolonies. This phenotype was named localized adherence by Scaletsky and colleagues (Scaletsky et al., 1984). After the initial stage of adherence, EPEC injects virulence molecules with the T3SS into the host causing the bacteria to adhere more vigorously and initiate the formation of A/E lesions (Moon et al., 1983). The damage leads to the retention of water and the malabsorption of nutrients and therefore to diarrhea and other symptoms. While the time frame of the onset of symptoms suggests that changes in chloride ion secretion are the *de facto* main cause of acute diarrhea (Lapointe et al., 2009), A/E lesions and the associated actin pedestals are considered to be important facets of the illness allowing for chronic infections lasting up to 30 days (Fagundes-Neto and Scaletsky, 2000).

Our assay focuses on the fact that EPEC effectors manipulate the cytoskeleton, inducing so-called actin pedestals, protrusions of abnormal actin polymerization. While the exact function of actin pedestals is unknown, they may be a form of niche construction and function to protect the pathogen from environmental stress, for example shear within the intestines, and host immune responses such as phagocytosis (for discussion on theories of possible function see, for example Battle et al., 2014; Brady, 2007; Cepeda-Molero et al., 2020). Compounds or structural motifs capable of altering the actin polymerization phenotypes caused by bacterial pathogens, could be used as starting points for the development of antivirulence drugs especially since deletion mutants lacking some of the effectors involved tend to show either attenuated virulence or the lack of it entirely. For example, the deletion of EPEC *eae* – a gene encoding a C-lectin adhesin intimin, expressed on the bacterial outer membrane and responsible for binding to a translocated receptor, Tir – produces mutants incapable of forming pathogenic actin rearrangements and showing decreased adhesion in cell culture models (Cleary, 2004), although in cultured human biopsies other effectors are also required (Cepeda-Molero et al., 2017). Similarly, the deletion of *espA,* a gene encoding one of the main structural proteins of the T3SS appendage, produce mutants showing decreased adhesion to cells (Cleary, 2004).

To our knowledge, high-throughput assays monitoring pathogen-induced actin rearrangements have not been reported before. We therefore designed a high-content fluorescence-based imaging assay using the previously described fluorescent actin staining assay (Knutton et al., 1989), a fluorescent EPEC strain, and readily available license-free image analysis software. This assay is capable of assessing the capacity of compounds to inhibit A/E lesion-associated actin rearrangement.

2. Materials and methods

2.1. Assay design

The overall workflow of the assay is shown in Fig. 1. The assay in its entirety can be run in two days, where the first day is required for preparation of cell and bacterial cultures. On the second day the infection, staining, and imaging are done. After the plates are fixed, they can be stored without considerable degradation for at least a week in the dark at +4 °C until imaging is performed.

2.1.1. Creation and validation of the fluorescent bacterial strain

Escherichia coli 2348/69, a typical EPEC type 1 strain, was obtained from Reference Microbiology Services, UK. Liquid overnight cultures were grown in LB broth at 37 °C and 200 rpm from single colonies taken from a weekly renewed LB agar culture. For image acquisition, the strain was transformed with a plasmid to constitutively express fluorescent protein mCherry. To achieve this, competent bacteria were made using the rubidium chloride method (Bird, 2011). The plasmid pON.mCherry, Addgene #84821 deposited by Howard Schuman (Gebhardt et al., 2017), was extracted using a miniprep kit (GeneJET, Thermo Fisher Scientific K0502). After this, the extracted plasmid was incubated with the competent bacteria and the transformants were selected with 30 μg mL^{-1} chloramphenicol and deposited into long-term storage (−80 °C) as glycerol stocks.

To assess stability of the fluorescent strain, we proliferated and incubated the transformed bacteria in conditions identical to those used in the assay. After pre-incubation in MEM, 100 μL suspensions (2×10^6 cfu mL^{-1}) of bacteria were placed into an empty imaging 96-well plate

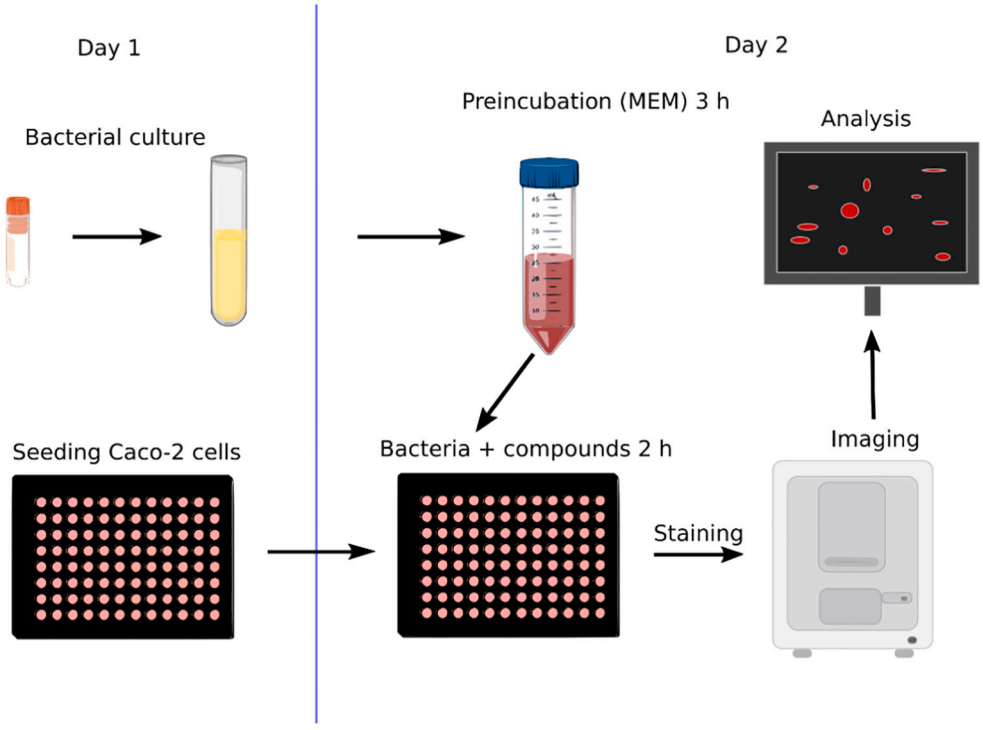

Fig. 1. The assay workflow. On the first day, Caco-2 cells are seeded to a well plate while an overnight liquid culture is initiated from the glycerol stock of the bacteria. The following day, bacteria are first preincubated in serum-free MEM for three hours and used to infect the cells. The cells are then incubated with the bacteria for two hours and exposed to test compounds or the aurodox control. The infection is terminated by adding the fixative-containing staining solution, after which the plate is imaged, and the images processed.

(Viewplate, Perkin Elmer) where they were imaged with phase contrast and fluorescence microscopy at 20×. The resulting images were processed principally following the ideas described by Canny (1986) and enumerating the individual bacteria in both the phase contrast and the fluorescence image to estimate the proportion of fluorescent bacteria in the population.

To demonstrate that the transformed EPEC strain pertained pathogenicity, we infected the cells with the transformed strain and the wild type side-by-side using antibodies to visualize the non-fluorescent bacteria. Cells infected with non-fluorescent wild type bacteria were first washed three times with Hank's Balanced Salt solution (HBSS), and fixed in 4% paraformaldehyde for ten minutes. The cells were then washed thrice with PBS and blocked using 1% bovine serum albumin (Merck) for one hour. After this, the cells were permeabilized with 0.1% (*v*/v) Triton X-100 and 1% (*w*/*v*) BSA in PBS for three minutes and washed thrice with PBS. Next, the samples were incubated with *E. coli* serotype O/K polyclonal antibody (PA1-73032, Thermo Fisher Scientific) 1:100 and 1% BSA for two hours. The cells were washed thrice with PBS, then incubated with Rabbit anti-goat IgG (H + L) Cross-Adsorbed antibody conjugated to AlexaFluor-594 (Thermo Fisher Scientific) 1:1000 and 1% BSA, for one hour, and washed with PBS thrice. For the analysis of F-actin, AlexaFluor-488-conjugated phalloidin (Thermo Fisher Scientific) was applied (20 pM) for 20 min and for nuclei Hoechst 333432 (Merck) (3 μg/mL) for three minutes. Then cells were washed three times with PBS before imaging. All these steps were performed at room temperature.

2.1.2. Infection of mammalian cells

Human epithelial colorectal adenocarcinoma Caco-2 cells (ATCC HTB-37) were maintained in Minimal Essential Medium (MEM) supplemented with 10% fetal bovine serum (FBS), 1% L-glutamine and 1% non-essential amino acids at 37 °C, 95% humidity and 5% CO_2. All cell culture reagents were obtained from Thermo Fisher Scientific.

The infection of Caco-2 cells was performed essentially as described previously (Cravioto et al., 1979; Knutton et al., 1989). The cells were seeded onto poly-D-lysine (Merck) coated, black, clear bottom 96-well plates (Viewplate, Perkin Elmer) at 4×10^4 cells per well and incubated for 24 h before the infection. Overnight bacterial liquid cultures were proliferated directly from the glycerol stocks, by cultivation in sterile glass tubes in LB broth supplemented with 30 μg mL^{-1} chloramphenicol at 37 °C, 200 rpm. Bacteria were then preincubated as described previously (Vuopio-Varkila and Schoolnik, 1991) in a nutrient-deficient medium (MEM without serum) to promote the expression of virulence factors including bundle forming pili (Vuopio-Varkila and Schoolnik, 1991) and locus of enterocyte effacement (LEE) gene products (Hazen et al., 2017). Liquid overnight cultures were diluted 1:50 in serum-free MEM and placed for three hours at 37 °C without shaking in a centrifuge tube with filter cap (Corning mini bioreactor 431,720). At this point, we also added the positive control, aurodox (1–10 μg mL^{-1}) (BioVision), into one of the bioreactors. Finally, the preincubated bacteria were added to the well plates at a multiplicity of infection (MOI) of 1:10 suspended in serum-free MEM. The plates were centrifuged (Eppendorf 5840R) for four min at 1000 ×g for the synchronization of the infection, and subsequently incubated for two hours at 37 °C and 5% CO_2.

2.1.3. Fluorescence staining

Cells infected with the mCherry-expressing EPEC were fixed and stained following a protocol published earlier (Knutton et al., 1989), with slight modifications to make it more amenable for high-throughput assays. An equivalent volume (100 μL) of staining solution [8% paraformaldehyde, 0.2% Triton-X (Thermo Fisher Scientific), 40 pM phalloidin-AlexaFluor-488 (Thermo Fisher Scientific), 6 μg/mL Hoechst 33342 (Thermo Fisher Scientific) in PBS] was added directly to the incubation medium for 20 min. The cells were washed three times with HBSS before imaging.

2.1.4. Imaging

After the cells were infected and stained as described above, they were imaged using Cytation 5 (BioTek) with 20× Plan Fluorite phase contrast NA 0.45 objective (Olympus 1,320,517) and filter cubes for DAPI (1225100) to visualize Hoechst 33342, Texas red (1225102) to visualize mCherry and GFP (1225101) to visualize AlexaFluor-488. Focal plane stacks of 20 images with distance 0.8 μm of each other were taken from five non-overlapping fields of view within each well. The locations of these were the same for each well as the microscope does not allow imaging at random locations. A stack of focal planes and their projection was used to ensure capturing in-focus actin pedestal images over the entire field of view as the pedestals are not always entirely on the same z-plane. We used three of the images from the stack for the projection, the rest of the – mostly out-of-focus – stack images were excluded from the analysis. Taking such excessive image stacks is due to a limitation of the imager, which does not allow to take a focal plane stack of three images from different focal points for the three different channels separately. Data was reduced from all five fields of view and an arithmetic mean was calculated to represent the data for a particular well. More than one field allows for a better estimate of the well-level effect and also protects against failures in image acquisition as the probability of one image capture failing is substantially larger than that of five independent captures.

2.1.5. Image preprocessing and analysis

The raw images were preprocessed and analyzed using scikit-image 0.17 (van der Walt et al., 2014). The preprocessing stage consists of an algorithm which estimates the quality of the images before proceeding to the analysis. This includes the estimation of the degree to which cells occupy each field of view (confluency of the monolayer) and evaluates how well the autofocus algorithm of the microscope worked. Confluency is estimated by comparing the total image pixel count to the actin-stained areas that can display fluorescence signal, as this approaches 100% when there is an intact monolayer over the entire image. Bacteria bind to the plate giving misleading readouts if there are areas void of cells, since they cannot cause actin pedestals there. Similarly, out-of-focus images are detected by the "variance of the Laplacian"-method from the bacterial signal (International Conference on Pattern Recognition et al., 2000). Sometimes the autofocus algorithm of the imager would focus on a floating detached cell or debris or fail for no obvious reason. The captured image is convolved with a 10 × 10 Laplacian kernel to acquire the second derivative of the image and the variance of the transform is measured. Properly focused images generally have higher variance because of sharp contrasts, whereas images with issues in focus, such as blur, will have lower than expected values. Low quality images were then flagged and automatically removed, as they were rare events. Low quality was defined as either more than 10% of the image missing cells or a variance of the Laplacian more than three standard deviations from the mean. When an image was rejected in this manner, it meant that the well-level data was produced by averaging only four, and not five, fields of view for one well. In other words, no well level data was deleted or marked as an outlier as is often done in screening.

A set of features was extracted from the preprocessed images. The microcolony counts were extracted by first uncovering a threshold value via Otsu's method, which minimizes interclass intensity variance for signal and background (Otsu, 1979). Subsequently, this threshold value was used to create a binary (foreground/background) mask, which was then used for labeling all connected components from the bacterial signal with a Union Find algorithm and counting each object (Fiorio and Gustedt, 1996)(depicted in Fig. 2A).

To enumerate the pedestals, we applied the created binary mask to the image of the actin staining captured from the equivalent location to define regions of interest (Fig. 2B) and saved them as individual images (examples in Fig. 2C). These collections of segments from each field of view were then subjected to further analysis, where contours were

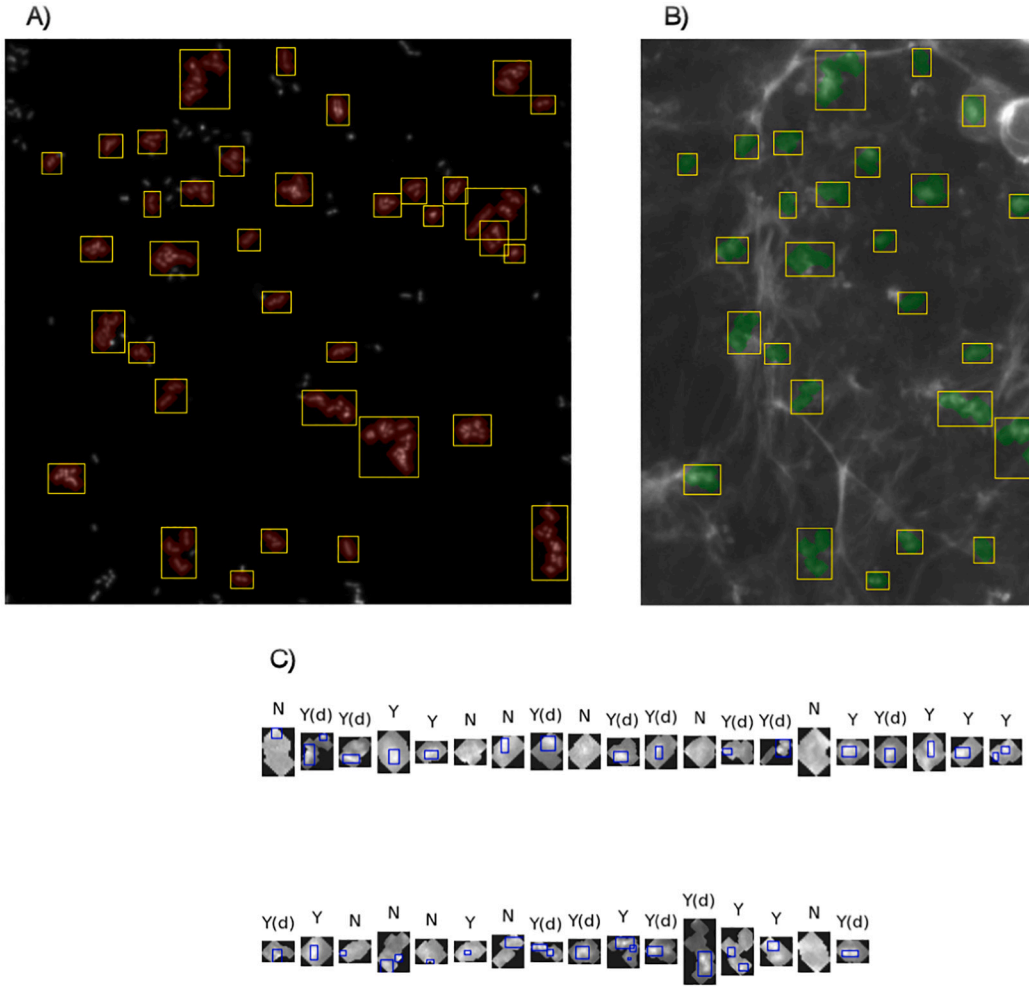

Fig. 2. Image processing methods. A) First, a mask is created from the fluorescence signal emitted by the bacteria (mCherry). The mask is shown in red and corresponds to the areas where the microcolonies are located. B) Then the equivalent regions are cut out from the actin signal in the primary segmentation step (phalloidin stained image). C) Lastly, secondary segmentation is performed within the collected primary segments, here marked with a blue bounding box. Images classified Y = pedestal, N = not, d = dense as described in section 2.1.5. These images are cropped for presentation. (For interpretation of the references to color in this figure legend, the reader is referred to the web version of this article.)

searched for from within them by tracking the most intense pixels by another round of segmentation (Fig. 2C). This is based on the notion that actin pedestals are excessive polymerization of actin, which would lead to higher local concentrations of the fluorophores. If these secondary segments from within the primary segments were co-located with a microcolony – that is they also had higher than threshold fluorescence from the equivalent region in the bacterial signal – they were kept and counted as pedestals, otherwise they were discarded as artifacts or other actin condense structures not related to bacteria. After summing up all the colonies and pedestals in this way, they were combined into a descriptive proportion number $\hat{p}(x)$, by dividing the amount of pedestals (all segments, s_i that meet the conditions x for being a pedestal) by the amount of colonies (n):

$$\hat{p}(x) = \frac{1}{n}\sum_{i}^{n} |s_i = x|$$

In addition, we measured bulk fluorescence, microcolony size and density of the pedestals, estimated by computing the distance from the minimum to maximum intensity within the saved individual images (shown in Fig. 2C).

Plotting was performed using the graphing tool, GR with the StatsPlots library of Julia, and scientific color maps (Crameri, 2019). Statistics were calculated with libraries of Julia 1.6 (Bezanson et al., 2017).

2.1.6. Selection of the positive control

The assay protocol was executed as described above (see 2.1) while various candidate compounds were added in a range of concentrations (Table 1). Aurodox was administered in advance as explained above (see 2.1.2) while other substances were administered to the bacteria upon infecting the cells. For selection we used a random intercept and random slope linear mixed effects model to detect any monotonic concentration-dependent response and evaluate the intraclass correlation of the measurements within the experiments. As selection criteria we used the

Table 1
Compounds considered as positive controls for the assay.

Control compound	Concentrations	Proposed mechanism of action	Source
aurodox (Kimura et al., 2011)	0.1–10 μg mL^{-1}	down-regulation of LEE-genes	BioVision
lactoferrin human, recombinant, (rice), iron saturated, ≥90% (Ochoa et al., 2003)	5–20 mg mL^{-1}	multiple mechanisms; preventing needle complex	Merck
peptide (YFPYSHTSPRQP) (Li et al., 2016)	50–200 μg mL^{-1}	blocking of EspB	Merck
genistein	16–67 μg mL^{-1}	kinase inhibitor	Merck

model slope and between-experiment variability (Supplementary data Table S1).

2.2. Assay validation

2.2.1. DMSO tolerance

As library compounds are often stored and administered to assays in DMSO, an experiment was carried out to assess the effects of DMSO on assay readouts. The assay protocol was executed as described above (see 2.1). Various concentrations (1–10%) of DMSO were added into the bacterial suspension for the duration of the infection.

2.2.2. Aurodox tolerance

Because the positive control was reported to have antimicrobial effects (Kimura et al., 2011; Maehr et al., 1979), an experiment was carried out to assess its capacity to inhibit bacterial growth. Bacteria were grown overnight and preincubated as described in 2.1.2. A suspension of about 4×10^6 bacteria /mL was prepared into fresh LB broth with chloramphenicol, dispensed into a white 96-well plate (100 µl/well) and exposed to different concentrations (2.5–10 µg mL^{-1}) of aurodox, to LB as a non-treated control and to 70 µg mL^{-1} streptomycin sulfate. After two hours, bacterial titer was assessed with an ATP-based kit BacTiter-Glo (Promega) measuring luminescence for 1000 ms on Varioskan LUX (Thermo Fisher Scientific).

2.2.3. Assay reproducibility

To evaluate the reproducibility of the assay between distinct days and variation between the wells within one individual plate, we followed the Assay Guidance Manual (Iversen et al., 2004). The assay was performed on three separate days by plating a maximal concentration (5.0 µg mL^{-1}) of the positive control aurodox, a lower concentration (2.5 µg mL^{-1}), and non-treated control at varying locations on the plate. After incubation, these plates were stained, imaged and analyzed as described above (see 2.1). We used Z' and Signal Window (SW) as effect size and variance metrics to assess the responses of the screening assay:

$$Z' = 1 - \frac{\left(\hat{\sigma}_{max} + \hat{\sigma}_{min}\right)}{\left|\hat{\mu}_{max} + \hat{\mu}_{min}\right|}$$

$$SW = \frac{\hat{\mu}_{max} - \hat{\mu}_{min} - 3\left(\hat{\sigma}_{max} + \hat{\sigma}_{min}\right)}{\hat{\sigma}_{max}}$$

where μ_{max} is the arithmetic mean of the high value sample (no inhibition) and μ_{min} is the low value sample mean, σ is the sample standard deviation.

3. Results and discussion

In past years, traditional target-based high-throughput screening (HTS) for antimicrobials has been essentially unsuccessful. An analysis of 70 HTS campaigns conducted towards essential genes of bacteria at GlaxoSmithKline during 1995–2001 described an end result of no workable drug candidates (Payne et al., 2007). A similar later analysis (2001−2010) of 65 HTS campaigns by AstraZeneca also failed to produce any (Tommasi et al. 2015). The authors of the later paper opinion that among other things, such campaigns utilize very reductionist assays uncovering active structures either not being capable of entering bacteria or being effluxed by membrane pumps.

Issues such as this have led to increased interest in whole-cell assays where the critical capacity of compounds to reach the target is assessed already during screening. For example, in the absence of any known shared molecule to target with ligand-based design, multiple whole-cell screening assays have analyzed phenotypic changes to uncover small molecule T3SS-inhibitors, leading to many publications on the structure-activity relationships and chemical optimizations of analogic structures (Gu et al., 2015). Among these are, for example, salicylaldehyde hydrazones and analogs, which are capable of inhibiting T3SSs in multiple pathogenic species of *Yersinia*, multiple *Chlamydias*, *Salmonella* and EPEC (Kauppi et al., 2003; Gauthier et al., 2005; Negrea et al., 2007). Independently of each other, Kauppi et al. (2003) and Gauthier et al. (2005) discovered similar chemical structures capable of inhibiting T3SS in *Yersinia pseudotuberculosis* and EPEC. Kauppi et al. (2003) used a whole-cell reporter gene assay to screen 9400 compounds against *Yersinia pseudotuberculosis* T3SS and Gauthier et al. monitored EspB secretion from the T3SS of EPEC in culture using ELISA against 20,000 Maybridge compounds. Similarly, Pan et al. (2007) used an avirulent but luminant *Yersinia pestis* to screen 70,966 compounds, finding previously recognized compounds but also other ones with entirely new structures. Yet another similar high-throughput approach is the absorbance-based monitoring of T3SS-dependant red blood cells lysis first described by Warawa et al. (Warawa, Finlay, and Kenny 1999). Screening using this method has led to the rediscovery of the antibiotics aurodox and factumycin as down-regulators of the T3SS (Kimura et al., 2011).

In a similar fashion, our primary objective was to create a high-content screening assay for EPEC pedestal formation using a whole-cell infection model. Therefore, we designed an automated fluorescence-imaging assay in which cell monolayers are infected with bacteria, and an infection phenotype is monitored using actin binding fluorophores. This assay is an automated, 96-well plate adaptation of the EPEC-Caco-2 adherence and fluorescence microscopy assay described by Knutton et al. (1989) supplemented with a suitable positive control and data reduction method based on extracting actin pedestals from the images automatically in high-throughput.

3.1. Assay design and validation

Expressing foreign proteins – such as the fluorescent protein we used – in pathogens, can change important biological properties of the microorganism, in the worst case rendering the entire assay invalid. Therefore, we evaluated whether the transformed strain created for the assay can cause comparable actin rearrangements on the cells leading to similar assay readouts. For this purpose, cells were infected with both the wild type EPEC strain, and the transformed fluorescent strain and compared. Both strains could adhere to the Caco-2 monolayer in microcolonies, infect the cultured cells, and produce similar actin polymerization phenotypes and readouts (Supplementary data Figs. S1-S2). We also carried out an experiment to evaluate the stability of the fluorescent strain in the assay (Supplementary data Figs. S3-S5). The results show that on average about 93.7% ($CI_{95\%}$ 89.3% - 96.7%) of the bacteria can be perceived with fluorescence imaging. A small proportion of non-fluorescent bacteria may be present in the assay, although non-viable bacteria are lost in washing steps of the assay. However, our methodology only uses the fluorescence signal to create a mask for downstream processing and this does not require every single bacterium to be fluorescent.

Since several substances have been reported in the literature to be capable of preventing EPEC A/*E*-lesions in *in vitro* models, we studied if they could also prevent actin pedestals in our assay and be used as controls. Most of these substances work by perturbing the T3SS in some manner (see Table 1).

Recombinant human lactoferrin did not show any effect on pedestal formation ($\beta = -0.001$, $p = 0.7$, see Fig. 3) according to our results. Ochoa et al. reported that lactoferrin prevents actin pedestals "due to interference with the initial step in EPEC mammalian cell attachment" (Ochoa et al., 2003). This discrepancy may be explained by the fact that lactoferrin does not decrease the proportion of colonies with pedestals but does decrease the absolute counts of actin pedestals by preventing the initial attachment to cell monolayers. Ochoa et al. analyzed actin pedestals in HEp2 monolayers by counting the HEp2 cells as positive for actin pedestals if they had microcolonies of at least ten bacteria and

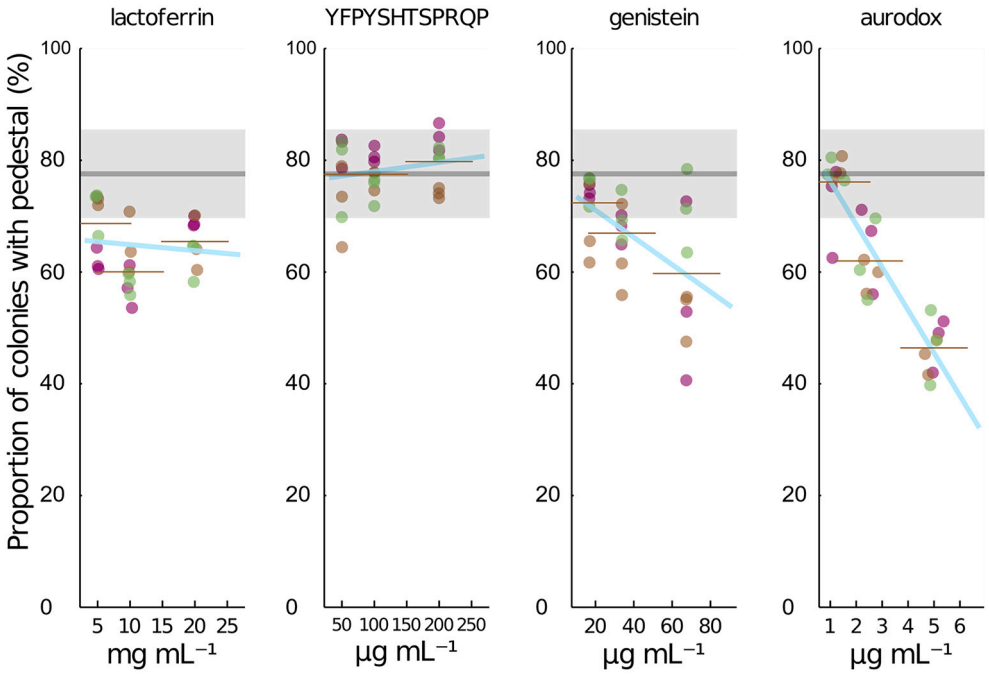

Fig. 3. The effects of positive control candidates on the proportion of colonies with pedestals in the assay. The peptide (YFPYSHTSPRQP) did not show any dose-dependent effect, lactoferrin had no effect on the readout, except that the intercept was slightly lower, due to it inhibiting normal colony formation. Genistein and aurodox displayed a dose-dependent decrease in the assay readout, though genistein demonstrated large between experiment variation. Data points represent means of five fields of view from three individual wells from three independent experiments performed on distinct days. The non-treated control (MEM only) is indicated in each panel as a grey line and a ribbon indicates the 95% confidence interval of the mean.

associated actin pedestals as evaluated by eye. They do not therefore address the issue of whether the microcolonies present display lesser relative degree of pedestal formation or not.

We noticed, additionally, that lactoferrin at 5.0 µg mL^{-1} did not decrease the total amount of bacteria present in the images, but rather it increased microcolony counts (230% compared to the non-treated control, Supplementary data Fig. S6) while decreasing microcolony average areas by 36% (Supplementary data Fig. S6). In contrast, compounds purely detrimental to microcolony formation – such as 10% DMSO – similarly decrease average sizes, but they also decrease total microcolony counts (Supplementary data Fig. S6). Interestingly microcolony sizes display a very uneven Pareto or exponential degree distribution, where the large majority have small sizes while a few colonies have large sizes. Indeed, this is what one would expect if bacterial aggregation to colonies displays preferential attachment and can be modelled with the Barabási–Albert model as most biological network phenomena can (Barabási, 2009; Grinberg et al., 2019). In other words, a new adhering or forming bacterium is likelier to appear in a colony with more members than into a small one. In any case, this also means that counting colonies above a certain size – such as that in the work of Ochoa et al. – will exclude more of the microcolonies in the lactoferrin condition than in other conditions not affecting the size. Thus, it is possible to see an increase in total microcolony counts, while simultaneously seeing a decrease in cells positive for actin pedestals. Ochoa et al. also used a four-hour incubation time and much higher MOI (1:500) than used in this work. Due to lactoferrin's capacity to change the localized adherence phenotype, the assay we describe here can be used to probe the effects of library compounds on microcolony formation using 5.0 mg mL^{-1} lactoferrin as a control.

A peptide (YFPYSHTSPRQP) reported to be capable of preventing localized adherence – an early attachment phenotype of some EPEC strains (Li et al., 2016) – resulted in no measurable decrease in the number of actin pedestals ($\beta = 0.0002$, $p = 0.19$, see Fig. 3). Neither did it have any effect on EPEC microcolony size nor counts (Supplementary data Fig. S6). Li et al. used a much shorter infection time (30 min) and did not analyze pedestals, but only adhesion.

Genistein, a kinase inhibitor used as a control in many assays involving actin rearranging pathogens (Coconnier et al., 1998; Rosenshine et al., 1996) was capable of preventing actin pedestals in our assay ($\beta = -0.002$ $p = 0.04$, see Fig. 3). There was, however, considerable variation between experiments, which perhaps are not due to properties inherent to genistein, but rather further optimization would be needed. The duration between pipetting the suspensions and the plate reaching the incubator likely needs to be very precise, since the effect of genistein is known to be enhanced by short pretreatment of the cells before infection. However, as genistein is a promiscuous kinase blocker with multiple other inhibiting effects on normal cell signaling, it also interferes with the normal biology of the host cell to some degree.

Aurodox – an antibiotic produced by *Streptomyces goldniensis* (Maehr et al., 1973, 1979) – is a member of the elfamycin family of antibiotics first described in the 1970's (Maehr et al., 1973). It was rediscovered as a T3SS inhibitor in 2011, in a screening campaign utilizing natural product libraries (Kimura et al., 2011). The exact mechanism of action of aurodox is not entirely understood, but like other antimicrobial substances extracted from *Streptomyces*, it inhibits protein biosynthesis, although through an elongation factor (Tu), and not by directly inhibiting ribosome activity (Parmeggiani and Swart, 1985; Vogeley et al., 2001). This down-regulates the transcription of T3SS-related genes in the locus of enterocyte effacement (LEE) via the repression of a master regulator (*ler*) (Elliott et al., 2000). These genes are known to be necessary for the induction of actin pedestals in *in vitro* organ culture (Cepeda-Molero et al., 2017). In our assay we pretreated bacteria with aurodox due to its translation-mediated mechanism of action. Aurodox both decreased the quantity of perceivable pedestals ($\beta = -0.076$, $p < 0.001$, see Fig. 3) and their density suggesting that it partially prevented actin condensation underneath the colonies. Aurodox at concentration of 5.0 µg mL^{-1} was used in earlier high-throughput assays (Kimura et al., 2011) and it only slightly inhibited the growth of the transformed bacteria (Supplementary data Fig. S7). We therefore chose aurodox at 5.0 µg mL^{-1} concentration as positive control for further assay validation steps.

Most screening library compounds are stored and delivered in DMSO. The ability of Caco-2 cells to tolerate DMSO concentrations up to 10% without substantial membrane damage or changes in apical membrane permeability has been reported in the literature (Da Violante et al., 2002). Therefore, we conducted an experiment to assess the tolerance of the assay to DMSO at 1–10% of the total volume. DMSO concentration did not significantly alter the readout, but at

concentrations above 5% cell detachment increased lowering the values and causing increased variation (Supplementary data Fig. S8). However, total fluorescence emitted by bacteria decreased in a concentration-dependent manner (Supplementary data Fig. S9) suggesting possible toxicity or degradation of the fluorescent protein. Thus, total DMSO concentrations in this assay should not exceed 5% of total well volume.

In order to assess assay stability over different plates and days, we ran nine assay plates – three separate plates on three separate days – and analyzed the data following procedure and the acceptance criteria described in the assay guidance manual (Iversen et al., 2004). The results show a consistent signal over different plate regions (Fig. 4). There were no considerable between-plates differences, nor any difference over the distinct days; all within-day and between-day fold shifts were below two. There was also low variance between wells, the intraplate coefficients of variance being under 0.2 for the primary readout on average, while the signal windows (SW) were above 2 for all plates.

We calculated the Z'-factors on the pedestal counts as this data is on a scale that is more suitable for Z' than a bound proportion of counts (Iversen et al., 2006; Sui and Wu, 2007). Z' was designed for traditional HTS readouts and is not so well suited for imaging assays (Iversen et al., 2004). On average our assay scored a Z'-factor of 0.44 with four production assay replicates and has a $\sigma_{max}/\sigma_{min}$ of 1.0. This is equivalent to a $T_{80\%} \geq 50$ of 56.1, meaning that at a cut-off for hit selection of 56% inhibition this assay will recognize 76.7% of all compounds truly inhibiting at more than 50%, while only 20% of the compounds identified as active will not truly inhibit by more than 50% (Bar and Zweifach, 2020). However, the level of required replicates can be decreased by either using higher concentration of aurodox as a control or increasing the cut-off level to proclaim a compound active.

In order to be able to automatically screen the images, we designed an image analysis pipeline written in Python, in which we counted the amounts of pedestals in the field of view. Because Caco-2 cells display congenital structures rich in actin, processing fluorescent actin staining images via mere segmentation is not optimal for this complex assay set-up. Since the relevant actin rich pedestal structures are located underneath adherent bacteria, we processed the images by using the bacterial signal as a mask on the actin image. This process focuses the analysis on a very small part of the entire image (a region of interest, depicted in Fig. 2C), thus making it more specific and less prone to include false positives compared to simple segmentation from the actin channel, while remaining computationally light. At times the regions of interest may contain other actin rich structures not related to bacteria, or that are present over the entire segment with higher signal than that caused by the pedestal. To deal with this issue, we added a third step where the captured segments were validated by allowing only those with concurrent mCherry signal. This for the most part avoids capturing actin rich areas that are not related to bacteria and allows to achieve an adequate assay signal window.

Additionally, the total fluorescence intensity signal window from minimum to maximum, from the actin staining was measured as an indicator of the density of the actin condensation at that region. This was done because our control substances were capable of not only decreasing the count of pedestals, but also their total density, and such a number gives a means to estimate qualitative degradation of the pedestal structures in a production screen, in addition to simply enumerating them. This is particularly important, as there might exist library compounds that interfere with the condensation in multiple distinct ways.

Data extracted from the multiple fields of view were then aggregated by calculating their arithmetic mean. We tested the effect of using multiple fields of view on both the error of the estimate and on the variation between wells, by calculating the standard error of the mean and assay variability related parameters from data derived from one field of view, then adding additional fields of view until the results converge. As expected, increasing the number of fields of view used for the estimate decreases the level of error with diminishing returns (Table 2). The average standard error of the mean for the main readout

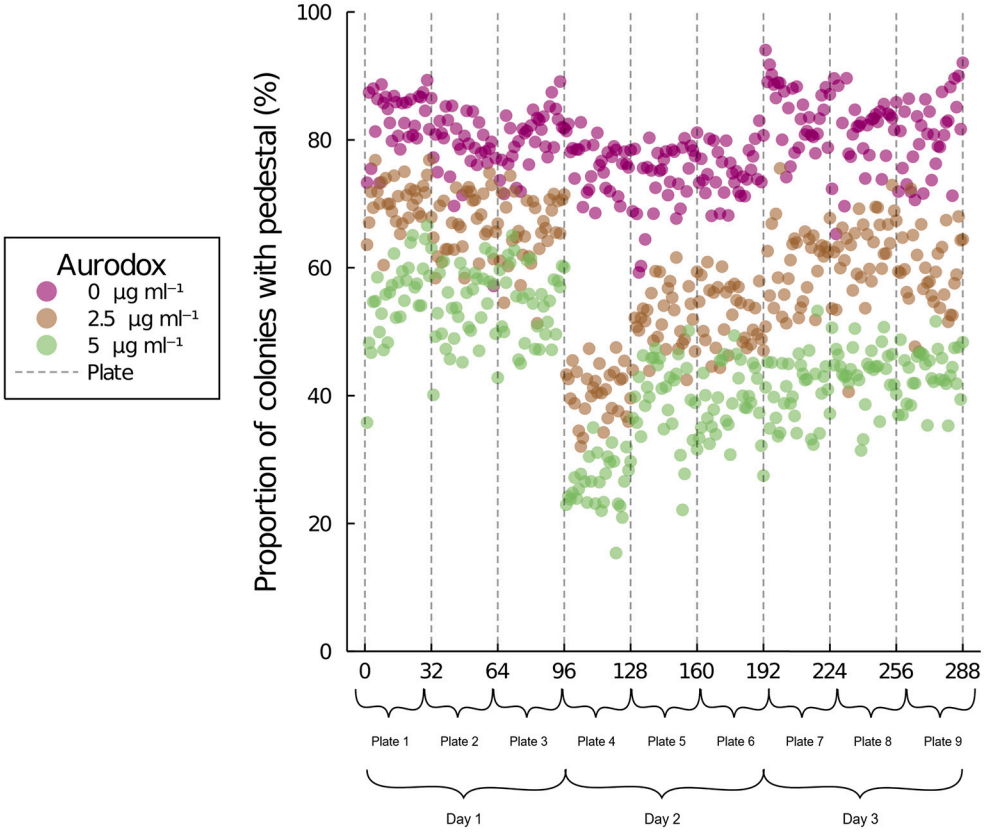

Fig. 4. Assay reproducibility over distinct plates and on various days. The plot shows results from three full 96-well plates on three distinct days (total of nine plates). The assay was performed by dispensing a maximal concentration (5.0 µg mL^{-1}) of the positive control aurodox, a lower concentration (2.5 µg mL^{-1}), and non-treated control (all with $8 \times 4 = 32$ wells) at varying locations on the plate, following guidelines of the Assay Guidance Manual (Sittampalam et al., 2004). Each data point represents an average measurement of five fields of view from one well.

Table 2
The number of fields of view decreases the error of the well level readout estimate, while increasing the signal window (SW) and Z' factor of the assay. These improvements are increasingly smaller in magnitude, however.

Number fields of view	SEM for well-level data	SW of plate	Z' of plate
Two	3.8	3.28	0.40
Three	3.0	4.82	0.48
Four	2.6	4.95	0.49
Five	2.5	4.35	0.47

decreased from 3.8 to 2.5 when moving from a mean of two fields of view to one of five, but the increment was smaller after each addition to the point that the last addition barely showed improvement (Supplementary data Fig. S10). The improved well-level estimate then decreased the between-well variation in such a manner that the SW and Z'-factor increased from 3.28 and 0.4 to 4.35 and 0.47, respectively. With five fields of view, the within-well coefficients of variation (CV) for the main readout were below 0.2 (Supplementary data Fig. S11).

3.2. Assay application areas

Above we discussed other whole-cell screening methods used to screen for T3SS inhibitors. While these do use whole-cell setups and wild type strains, they either do not model an actual infection of mammalian cells or analyze fairly crude endpoints, such as cell death or lysis. Our method is based on the monitoring of the phenotypic changes in the actin cytoskeleton, and therefore allows following the pathological changes to actin polymerization, in particular, in the case of some EPEC strains and their associated actin pedestals. In contrast to target-based assays, this phenotypic assay potentially allows to identify compounds interfering with a variety of target molecules involved in eliciting actin pedestals. In addition, pathogens may cause abnormal actin polymerization recognizable in images but nevertheless be incapable of red blood cell lysis or other effector-based damage to cells. Additionally, this assay can be used to monitor the earlier stages of EPEC adherence via following colony morphology and could be used to screen inhibitors of localized adherence and autoaggregation (Hyland et al., 2006). Obviously, however, imaging and the respective data analysis require specialized equipment and is more laborious. A limitation of our approach is that not all clinical EPEC isolates show actin polymerization in this assay *in vitro* (Knutton et al., 2001; Knutton et al., 1991). Such strains may nevertheless be pathogenic and cause A/E lesions *in vivo* (Rocha et al., 2011). One challenge of designing the assay was the selection of a positive control substance. Many substances are used in the literature for assays dealing with actin modulating pathogens or, alternatively, are known to prevent effector injection via the T3SS. Not all of them, however, are readily available or capable of creating a robust dose-dependent response via specific, non-lethal, effects preferably on the bacteria alone. While aurodox certainly can prevent actin pedestals, the bacteria need to be pretreated before-hand due to the translation-mediated mechanism of action. In most screening settings this is not, however, something that can be reasonably done when screening extensive numbers of compounds, and one is then restricted to searching for compounds of more rapid manners of inhibition.

Given that multiple pathogens cause A/E lesions or use other cytoskeletal manipulation, it might be possible to extend the assay described here to study these other pathogens (Stradal and Schelhaas, 2018). Pathogens capable of causing the A/*E*-lesion phenotype and associated actin pedestals include enteropathogenic *Escherichia coli*, enterohemorrhagic *Escherichia coli* (EHEC), *Escherichia albertii*, a murine specific strain *Citrobacter rodentium*, and rabbit enteropathogenic *Escherichia coli* (Yamamoto et al., 2017). EHEC strains, for example, also cause pedestals in cultured cells, although according to Knutton et al., they do not all attach to Caco-2 cells. The authors, however, also reported that EHEC strains of serotypes 0157:H7 and 026:H11 do adhere to Hep-2 and HEL cell monolayers, suggesting that these might be reasonable alternative host cells (Knutton et al., 1989). Various other abnormal actin accumulation phenotypes are described in the literature (Stevens et al., 2006). For example, "comet tails" created by *Listeria*, *Rickettsia*, *Bulkholderia*, (Ambrosi et al., 2012; Jasnin et al., 2013; Valvano et al., 2005) "ruffles" by *Salmonella* (Francis et al., 1993), and expanding the image analysis and classification algorithms to distinguish these phenotypes is possible. While aurodox, which is used here as a positive control, may not be suitable for use with other pathogens, salicylaldehyde hydrazones (Negrea et al., 2007) or actin polymerization disruptors, like cytochalasin D (Sanger et al., 1996) or tyrosine kinase inhibitors (staurosporine, genistein)(Benjamin et al., 1995), and possibly many more substances, can be substituted if needed.

3.3. Conclusions

Here we report the optimization and validation of HTS-compatible high-content imaging assay for screening for compounds inhibiting pathogen-induced actin pedestals. The method is based on a fluorescent EPEC strain accompanied by actin staining and therefore can be used for detecting molecules targeting effectors inducing actin pedestals in EPEC infection. With some modifications, this assay could be amended for studying other actin-modulating pathogens. The assay can be performed in 96-well format therefore enhancing the discovery of new anti-virulence compounds.

Funding

This work was supported by the Academy of Finland [grant numbers 312503 and 284477]

Declaration of Competing interest

Authors declare no competing interest.

Appendix A. Supplementary data

The code used for analysis publically available athttps://github.com/tpylkko/FAS-HCS/. Supplementary data to this article can be found online at https://doi.org/10.1016/j.mimet.2021.106201.

References

International Conference on Pattern Recognition, Sanfeliu, A., International Association for Pattern Recognition, 2000. Proceedings / 15th International Conference on Pattern Recognition: Barcelona, Spain, September 3–7, 2000. Presented at the International Conference on Pattern Recognition. IEEE Computer Society, Los Alamitos, Calif.

Ambrosi, C., Pompili, M., Scribano, D., Zagaglia, C., Ripa, S., Nicoletti, M., 2012. Outer membrane protein a (OmpA): a new player in *Shigella flexneri* protrusion formation and inter-cellular spreading. PLoS One 7, e49625. https://doi.org/10.1371/journal.pone.0049625.

Bar, H., Zweifach, A., 2020. Z' does not need to be > 0.5. SLAS. Discov. Adv. Sci. Drug Discov. 25, 1000–1008. https://doi.org/10.1177/2472555220942764.

Barabási, A.-L., 2009. Scale-free networks: a decade and beyond. Science 325, 412–413. https://doi.org/10.1126/science.1173299.

Baron, C., 2010. Antivirulence drugs to target bacterial secretion systems. Curr. Opin. Microbiol. 13, 100–105. https://doi.org/10.1016/j.mib.2009.12.003.

Battle, S.E., Brady, M.J., Vanaja, S.K., Leong, J.M., Hecht, G.A., 2014. Actin pedestal formation by Enterohemorrhagic *Escherichia coli* enhances bacterial host cell attachment and concomitant type III translocation. Infect. Immun. 82, 3713–3722. https://doi.org/10.1128/IAI.01523-13.

Benjamin, P., Federman, M., Wanke, C.A., 1995. Characterization of an invasive phenotype associated with enteroaggregative *Escherichia coli*. Infect. Immun. 63, 3417–3421. https://doi.org/10.1128/IAI.63.9.3417-3421.1995.

Bezanson, J., Edelman, A., Karpinski, S., Shah, V.B., 2017. Julia: a fresh approach to numerical computing. SIAM Rev. 59, 65–98. https://doi.org/10.1137/141000671.

Bird, L.E., 2011. High throughput construction and small scale expression screening of multi-tag vectors in *Escherichia coli*. Methods 55, 29–37. https://doi.org/10.1016/j.ymeth.2011.08.002.

Brady, M.J., 2007. Mechanism and Function of Actin Pedestal Formation by Enterohemorrhagic *Escherichia coli* O157:H7: A Dissertation. University of Massachusetts Medical School. https://doi.org/10.13028/ZJB9-1J13.

Buroni, S., Chiarelli, L.R., 2020. Antivirulence compounds: a future direction to overcome antibiotic resistance? Future Microbiol. 15, 299–301. https://doi.org/10.2217/fmb-2019-0294.
Canny, J., 1986. A computational approach to edge detection. IEEE Trans. Pattern Anal. Mach. Intell. 679–698. https://doi.org/10.1109/TPAMI.1986.4767851. PAMI-8.
Cepeda-Molero, M., Berger, C.N., Walsham, A.D.S., Ellis, S.J., Wemyss-Holden, S., Schüller, S., Frankel, G., Fernández, L.Á., 2017. Attaching and effacing (A/E) lesion formation by enteropathogenic *E. coli* on human intestinal mucosa is dependent on non-LEE effectors. PLOS Pathog. 13, e1006706. https://doi.org/10.1371/journal.ppat.1006706.
Cepeda-Molero, M., Schüller, S., Frankel, G., Ángel Fernández, L., 2020. Systematic deletion of type III secretion system effectors in Enteropathogenic *E. coli* unveils the role of non-LEE effectors in a/E lesion formation. In: E. Coli infection [working title]. IntechOpen. https://doi.org/10.5772/intechopen.91677.
Cleary, J., 2004. Enteropathogenic *Escherichia coli* (EPEC) adhesion to intestinal epithelial cells: role of bundle-forming pili (BFP), EspA filaments and intimin. Microbiology 150, 527–538. https://doi.org/10.1099/mic.0.26740-0.
Coconnier, M.H., Dlissi, E., Robard, M., Laboisse, C.L., Gaillard, J.L., Servin, A.L., 1998. *Listeria monocytogenes* stimulates mucus exocytosis in cultured human polarized mucosecreting intestinal cells through action of listeriolysin O. Infect. Immun. 66, 3673–3681.
Crameri, F., 2019. Scientific Colour Maps. Zenodo. https://doi.org/10.5281/ZENODO.3596401.
Cravioto, A., Gross, R.J., Scotland, S.M., Rowe, B., 1979. An adhesive factor found in strains of *Escherichia coli* belonging to the traditional infantile enteropathogenic serotypes. Curr. Microbiol. 3, 95–99. https://doi.org/10.1007/BF02602439.
Da Violante, G., Zerrouk, N., Richard, I., Provot, G., Chaumeil, J.C., Arnaud, P., 2002. Evaluation of the cytotoxicity effect of dimethyl sulfoxide (DMSO) on Caco2/TC7 colon tumor cell cultures. Biol. Pharm. Bull. 25, 1600–1603. https://doi.org/10.1248/bpb.25.1600.
Dickey, S.W., Cheung, G.Y.C., Otto, M., 2017. Different drugs for bad bugs: antivirulence strategies in the age of antibiotic resistance. Nat. Rev. Drug Discov. 16, 457–471. https://doi.org/10.1038/nrd.2017.23.
Elliott, S.J., Sperandio, V., Girón, J.A., Shin, S., Mellies, J.L., Wainwright, L., Hutcheson, S.W., McDaniel, T.K., Kaper, J.B., 2000. The locus of enterocyte effacement (LEE)-encoded regulator controls expression of both LEE- and non-LEE-encoded virulence factors in enteropathogenic and enterohemorrhagic *Escherichia coli*. Infect. Immun. 68, 6115–6126. https://doi.org/10.1128/iai.68.11.6115-6126.2000.
Eltai, N.O., Al Thani, A.A., Al Hadidi, S.H., Al Ansari, K., Yassine, H.M., 2020. Antibiotic resistance and virulence patterns of pathogenic *Escherichia coli* strains associated with acute gastroenteritis among children in Qatar. BMC Microbiol. 20, 54. https://doi.org/10.1186/s12866-020-01732-8.
Fagundes-Neto, U., 2013. Persistent diarrhea: still a serious public health problem in developing countries. Curr. Gastroenterol. Rep. 15, 345. https://doi.org/10.1007/s11894-013-0345-1.
Fagundes-Neto, U., Scaletsky, I.C.A., 2000. The gut at war: the consequences of enteropathogenic *Escherichia coli* infection as a factor of diarrhea and malnutrition. Sao Paulo Med. J. 118, 21–29. https://doi.org/10.1590/S1516-31802000000100006.
Fiorio, C., Gustedt, J., 1996. Two linear time union-find strategies for image processing. Theor. Comput. Sci. 154, 165–181. https://doi.org/10.1016/0304-3975(94)00262-2.
Francis, C.L., Ryan, T.A., Jones, B.D., Smith, S.J., Falkow, S., 1993. Ruffles induced by Salmonella and other stimuli direct macropinocytosis of bacteria. Nature 364, 639–642. https://doi.org/10.1038/364639a0.
Gauthier, A., Robertson, M.L., Lowden, M., Ibarra, J.A., Puente, J.L., Finlay, B.B., 2005. Transcriptional inhibitor of virulence factors in Enteropathogenic *Escherichia coli*. Antimicrob. Agents Chemother. 49, 4101–4109. https://doi.org/10.1128/AAC.49.10.4101-4109.2005.
Gebhardt, M.J., Jacobson, R.K., Shuman, H.A., 2017. Seeing red; the development of pON.mCherry, a broad-host range constitutive expression plasmid for Gram-negative bacteria. Plos One 12, e0173116. https://doi.org/10.1371/journal.pone.0173116.
Gophna, U., Ron, E.Z., Graur, D., 2003. Bacterial type III secretion systems are ancient and evolved by multiple horizontal-transfer events. Gene 312, 151–163. https://doi.org/10.1016/S0378-1119(03)00612-7.
Grinberg, M., Orevi, T., Kashtan, N., 2019. Bacterial surface colonization, preferential attachment and fitness under periodic stress. PLoS Comput. Biol. 15, e1006815 https://doi.org/10.1371/journal.pcbi.1006815.
Gu, L., Zhou, S., Zhu, L., Liang, C., Chen, X., 2015. Small-molecule inhibitors of the type III secretion system. Molecules 20, 17659–17674. https://doi.org/10.3390/molecules200917659.
Hazen, T.H., Michalski, J., Luo, Q., Shetty, A.C., Daugherty, S.C., Fleckenstein, J.M., Rasko, D.A., 2017. Comparative genomics and transcriptomics of *Escherichia coli* isolates carrying virulence factors of both enteropathogenic and enterotoxigenic *E. coli*. Sci. Rep. 7, 3513. https://doi.org/10.1038/s41598-017-03489-z.
Hyland, R.M., Griener, T.P., Mulvey, G.L., Kitov, P.I., Srivastava, O.P., Marcato, P., Armstrong, G.D., 2006. Basis for N-acetyllactosamine-mediated inhibition of enteropathogenic *Escherichia coli* localized adherence. J. Med. Microbiol. 55, 669–675. https://doi.org/10.1099/jmm.0.46344-0.
Iversen, P.W., Benoit, B., Yun-Fei, C., Guha, R., 2004. HTS assay validation. In: Assay Guidance Manual. Eli Lilly & Company and the National Center for Advancing Translational Sciences, Bethesda (MD).
Iversen, P.W., Eastwood, B.J., Sittampalam, G.S., Cox, K.L., 2006. A comparison of assay performance measures in screening assays: signal window, Z' factor, and assay variability ratio. J. Biomol. Screen. 11, 247–252. https://doi.org/10.1177/1087057105285610.
Jain, R., Beckett, V.V., Konstan, M.W., Accurso, F.J., Burns, J.L., Mayer-Hamblett, N., Milla, C., VanDevanter, D.R., Chmiel, J.F., 2018. KB001-A, a novel anti-inflammatory, found to be safe and well-tolerated in cystic fibrosis patients infected with *Pseudomonas aeruginosa*. J. Cyst. Fibros. 17, 484–491. https://doi.org/10.1016/j.jcf.2017.12.006.
Jasnin, M., Asano, S., Gouin, E., Hegerl, R., Plitzko, J.M., Villa, E., Cossart, P., Baumeister, W., 2013. Three-dimensional architecture of actin filaments in *Listeria monocytogenes* comet tails. Proc. Natl. Acad. Sci. 110, 20521–20526. https://doi.org/10.1073/pnas.1320155110.
Kauppi, A.M., Nordfelth, R., Uvell, H., Wolf-Watz, H., Elofsson, M., 2003. Targeting bacterial virulence. Chem. Biol. 10, 241–249. https://doi.org/10.1016/S1074-5521(03)00046-2.
Kimura, K., Iwatsuki, M., Nagai, T., Matsumoto, A., Takahashi, Y., Shiomi, K., Omura, S., Abe, A., 2011. A small-molecule inhibitor of the bacterial type III secretion system protects against in vivo infection with *Citrobacter rodentium*. J. Antibiot. (Tokyo) 64, 197–203. https://doi.org/10.1038/ja.2010.155.
Knutton, S., Baldwin, T., Williams, P.H., McNeish, A.S., 1989. Actin accumulation at sites of bacterial adhesion to tissue culture cells: basis of a new diagnostic test for enteropathogenic and enterohemorrhagic *Escherichia coli*. Infect. Immun. 57, 1290–1298.
Knutton, S., Phillips, A.D., Smith, H.R., Gross, R.J., Shaw, R., Watson, P., Price, E., 1991. Screening for enteropathogenic *Escherichia coli* in infants with diarrhea by the fluorescent-actin staining test. Infect. Immun. 59, 365–371. https://doi.org/10.1128/IAI.59.1.365-371.1991.
Knutton, S., Shaw, R., Phillips, A.D., Smith, H.R., Willshaw, G.A., Watson, P., Price, E., 2001. Phenotypic and genetic analysis of diarrhea-associated *Escherichia coli* isolated from children in the United Kingdom. J. Pediatr. Gastroenterol. Nutr. 33, 32–40. https://doi.org/10.1097/00005176-200107000-00006.
Lapointe, T.K., O'Connor, P.M., Buret, A.G., 2009. The role of epithelial malfunction in the pathogenesis of enteropathogenic *E. coli*-induced diarrhea. Lab. Investig. 89, 964–970. https://doi.org/10.1038/labinvest.2009.69.
Lee, V.T., Smith, R.S., Tümmler, B., Lory, S., 2005. Activities of *Pseudomonas aeruginosa* effectors secreted by the type III secretion system in vitro and during infection. Infect. Immun. 73, 1695–1705. https://doi.org/10.1128/IAI.73.3.1695-1705.2005.
Li, D., Chen, Z., Cheng, H., Zheng, J., Pan, W., Yang, W., Yu, Z., Deng, Q., 2016. Inhibition of adhesion of Enteropathogenic *Escherichia coli* to HEp-2 cells by binding of a novel peptide to EspB protein. Curr. Microbiol. 73, 361–365. https://doi.org/10.1007/s00284-016-1070-4.
Maehr, H., Leach, Michael, Yarmchuk, Linda, Stempel, Arthur, 1973. Antibiotic X-5108. V. Structures of antibiotic X-5108 and mocimycin. J. Am. Chem. Soc. 95, 8449–8450. https://doi.org/10.1021/ja00806a043.
Maehr, H., Leach, M., Yarmchuk, L., Mitrovic, M., 1979. Antibiotic X-5108. IX. Chemical conversion of mocimycin to aurodox and derivatives of aurodox, goldinamine and mocimycin. J. Antibiot. (Tokyo) 32, 361–367. https://doi.org/10.7164/antibiotics.32.361.
Mattoo, S., Lee, Y.M., Dixon, J.E., 2007. Interactions of bacterial effector proteins with host proteins. Curr. Opin. Immunol. 19, 392–401. https://doi.org/10.1016/j.coi.2007.06.005.
Moon, H.W., Whipp, S.C., Argenzio, R.A., Levine, M.M., Giannella, R.A., 1983. Attaching and effacing activities of rabbit and human enteropathogenic *Escherichia coli* in pig and rabbit intestines. Infect. Immun. 41, 1340–1351. https://doi.org/10.1128/IAI.41.3.1340-1351.1983.
Negrea, A., Bjur, E., Ygberg, S.E., Elofsson, M., Wolf-Watz, H., Rhen, M., 2007. Salicylidene Acylhydrazides that affect type III protein secretion in *Salmonella enterica* Serovar typhimurium. Antimicrob. Agents Chemother. 51, 2867–2876. https://doi.org/10.1128/AAC.00223-07.
Ochoa, T.J., Noguera-Obenza, M., Ebel, F., Guzman, C.A., Gomez, H.F., Cleary, T.G., 2003. Lactoferrin impairs type III secretory system function in Enteropathogenic *Escherichia coli*. Infect. Immun. 71, 5149–5155. https://doi.org/10.1128/IAI.71.9.5149-5155.2003.
Otsu, N., 1979. A threshold selection method from gray-level histograms. IEEE Trans. Syst. Man Cybern. 9, 62–66. https://doi.org/10.1109/TSMC.1979.4310076.
Pan, N., Goguen, J., Lee, C., 2007. High throughput screening for small-molecule inhibitors of type III secretion in *Yersinia pestis*. In: Perry, R.D., Fetherston, J.D. (Eds.), The Genus Yersinia. Springer New York, New York, NY, pp. 367–375. https://doi.org/10.1007/978-0-387-72124-8_34.
Parmeggiani, A., Swart, G.W., 1985. Mechanism of action of kirromycin-like antibiotics. Annu. Rev. Microbiol. 39, 557–577. https://doi.org/10.1146/annurev.mi.39.100185.003013.
Payne, D., Gwynn, M.N., Holmes, D.J., Pompliano, D.L., 2007. Drugs for bad bugs: confronting the challenges of antibacterial discovery. Nat. Rev. Drug Discov. 6, 29–40. https://doi.org/10.1038/nrd2201.
Rocha, S.P.D., Abe, C.M., Sperandio, V., Bando, S.Y., Elias, W.P., 2011. Atypical enteropathogenic *Escherichia coli* that contains functional locus of enterocyte effacement genes can be attaching-and-effacing negative in cultured epithelial cells. Infect. Immun. 79, 1833–1841. https://doi.org/10.1128/IAI.00693-10.
Rodrigues, R.S., Lima, N.C., Taborda, R.L.M., Esquerdo, R.P., Gama, A.R., Nogueira, P.A., Orlandi, P.P., Matos, N.B., 2019. Antibiotic resistance and biofilm formation in children with Enteropathogenic *Escherichia coli* (EPEC) in Brazilian Amazon. J. Infect. Dev. Ctries. 13, 698–705. https://doi.org/10.3855/jidc.10674.
Rosenshine, I., Ruschkowski, S., Stein, M., Reinscheid, D.J., Mills, S.D., Finlay, B.B., 1996. A pathogenic bacterium triggers epithelial signals to form a functional bacterial receptor that mediates actin pseudopod formation. EMBO J. 15, 2613–2624.

Sanger, J.M., Chang, R., Ashton, F., Kaper, J.B., Sanger, J.W., 1996. Novel form of actin-based motility transports bacteria on the surfaces of infected cells. Cell Motil. Cytoskeleton 34, 279–287. https://doi.org/10.1002/(SICI)1097-0169(1996)34:4<279::AID-CM3>3.0.CO;2-3.

Scaletsky, I.C., Silva, M.L., Trabulsi, L.R., 1984. Distinctive patterns of adherence of enteropathogenic *Escherichia coli* to HeLa cells. Infect. Immun. 45, 534–536. https://doi.org/10.1128/IAI.45.2.534-536.1984.

Sittampalam, G., Grossman, A., Brimacombe, K. (Eds.), 2004. Assay Guidance Manual. Eli Lilly & Company and the National Center for Advancing Translational Sciences, Bethesda (MD).

Stevens, J.M., Galyov, E.E., Stevens, M.P., 2006. Actin-dependent movement of bacterial pathogens. Nat. Rev. Microbiol. 4, 91–101. https://doi.org/10.1038/nrmicro1320.

Stradal, T.E.B., Schelhaas, M., 2018. Actin dynamics in host–pathogen interaction. FEBS Lett. 592, 3658–3669. https://doi.org/10.1002/1873-3468.13173.

Sui, Y., Wu, Z., 2007. Alternative statistical parameter for high-throughput screening assay quality assessment. J. Biomol. Screen. 12, 229–234. https://doi.org/10.1177/1087057106296498.

Theuretzbacher, U., Outterson, K., Engel, A., Karlén, A., 2020. The global preclinical antibacterial pipeline. Nat. Rev. Microbiol. 18, 275–285. https://doi.org/10.1038/s41579-019-0288-0.

Tommasi, Ruben, Brown, Dean G., Walkup, Grant K., Manchester, John I., Miller, Alita A., 2015. ESKAPEing the Labyrinth of Antibacterial Discovery. Nature Reviews Drug Discovery 14 (8), 529–542. https://doi.org/10.1038/nrd4572.

Valvano, M.A., Keith, K.E., Cardona, S.T., 2005. Survival and persistence of opportunistic *Burkholderia* species in host cells. Curr. Opin. Microbiol. 8, 99–105. https://doi.org/10.1016/j.mib.2004.12.002.

Vogeley, L., Palm, G.J., Mesters, J.R., Hilgenfeld, R., 2001. Conformational change of elongation factor Tu (EF-Tu) induced by antibiotic binding: crystal structure of the complex betwEEN EF-Tu·GDP and aurodox. J. Biol. Chem. 276, 17149–17155. https://doi.org/10.1074/jbc.M100017200.

Vuopio-Varkila, J., Schoolnik, G.K., 1991. Localized adherence by enteropathogenic *Escherichia coli* is an inducible phenotype associated with the expression of new outer membrane proteins. J. Exp. Med. 174, 1167–1177. https://doi.org/10.1084/jem.174.5.1167.

van der Walt, S., Schönberger, J.L., Nunez-Iglesias, J., Boulogne, F., Warner, J.D., Yager, N., Gouillart, E., Yu, T., scikit-image contributors, 2014. scikit-image: image processing in Python. PeerJ 2, e453. https://doi.org/10.7717/peerj.453.

Warawa, J., Finlay, B.B., Kenny, B., 1999. Type III Secretion-Dependent Hemolytic Activity of Enteropathogenic Escherichia Coli. Infection and Immunity 67 (10), 5538–5540.

Yamamoto, D., Hernandes, R.T., Liberatore, A.M.A., Abe, C.M., de Souza, R.B., Romão, F. T., Sperandio, V., Koh, I.H., Gomes, T.A.T., 2017. *Escherichia albertii*, a novel human enteropathogen, colonizes rat enterocytes and translocates to extra-intestinal sites. PLoS One 12, e0171385. https://doi.org/10.1371/journal.pone.0171385.